Science of the Total Environment 895 (2023) 165190

Contents lists available at ScienceDirect

Science of the Total Environment

journal homepage: www.elsevier.com/locate/scitotenv

# Vertical distribution and transport of microplastics in the urban atmosphere: New insights from field observations

Zhen Yuan [a,f], Cheng-Lei Pei [b], Heng-Xiang Li [a,c], Lang Lin [a,c], Rui Hou [a,c], Shan Liu [a,c], Kai Zhang [d], Ming-Gang Cai [e], Xiang-Rong Xu [a,c,*]

[a] Key Laboratory of Tropical Marine Bio-resources and Ecology, Guangdong Provincial Key Laboratory of Applied Marine Biology, South China Sea Institute of Oceanology, Chinese Academy of Sciences, Guangzhou 510301, China
[b] Guangzhou Sub-branch of Guangdong Ecological and Environmental Monitoring Center, Guangzhou 510006, China
[c] Sanya Institute of Ocean Eco-Environmental Engineering, Sanya 572100, China
[d] National Observation and Research Station of Coastal Ecological Environments in Macao, Macao Environmental Research Institute, Macau University of Science and Technology, Macao SAR, China
[e] State Key Laboratory of Marine Environmental Science, Xiamen University, Xiamen 361102, China
[f] University of Chinese Academy of Sciences, Beijing 100049, China

## HIGHLIGHTS

- Tower observations delineate vertical profile of atmospheric microplastics.
- Atmospheric microplastic abundance decreases with increasing height.
- PET and rayon fibers are the most prevalent types of atmospheric microplastics.
- Atmospheric stability and wind speed affect the vertical transport of atmospheric microplastics.
- The vertical transport of atmospheric microplastics is limited between 118 and 168 m.

## GRAPHICAL ABSTRACT

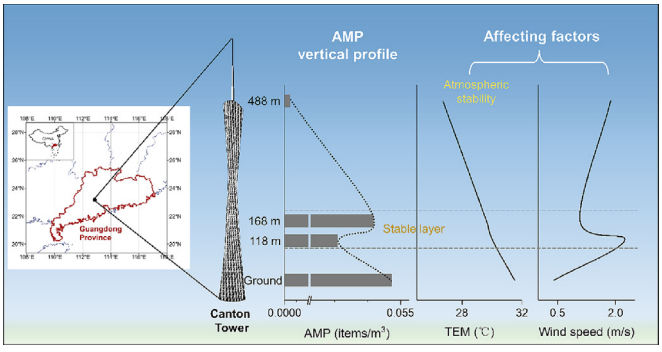


## ARTICLE INFO

Editor: Damia Barcelo

*Keywords:*
Atmospheric microplastics
Vertical profile
Atmospheric stability
Atmospheric boundary layer

## ABSTRACT

The distribution and transport of atmospheric microplastics (AMPs) have raised concerns regarding their potential effects on the environment and human health. Although previous studies have reported the presence of AMPs at ground level, there is a lack of comprehensive understanding of their vertical distribution in urban environments. To gain insight into the vertical profile of AMPs, field observations were conducted at four different heights (ground level, 118 m, 168 m and 488 m) of the Canton Tower in Guangzhou, China. Results showed that the profiles of AMPs and other air pollutants had similar layer distribution patterns, although their concentrations differed. The majority of AMPs were composed of polyethylene terephthalate and rayon fibers ranging from 30 to 50 μm. As a result of atmospheric thermodynamics, AMPs generated at ground level were only partially transported upward, leading to a decrease in their abundance with increasing altitude. The study found that the stable atmospheric stability and lower wind speed between 118 m and 168 m resulted in the formation of a fine layer where AMPs tended to accumulate instead of being transported upward. This study for the first time delineated the vertical profile of AMPs within the atmospheric boundary layer, providing valuable data for understanding the environmental fate of AMPs.

* Corresponding author at: Key Laboratory of Tropical Marine Bio-resources and Ecology, Guangdong Provincial Key Laboratory of Applied Marine Biology, South China Sea Institute of Oceanology, Chinese Academy of Sciences, Guangzhou 510301, China.
*E-mail address:* xuxr@scsio.ac.cn (X.-R. Xu).

http://dx.doi.org/10.1016/j.scitotenv.2023.165190
Received 25 April 2023; Received in revised form 19 June 2023; Accepted 26 June 2023
Available online 28 June 2023

## 1. Introduction

Microplastic (MP, <5 mm) is of great concern as an emerging contaminant. In recent years, atmospheric microplastics (AMPs) have been ubiquitous in the air, especially in urban areas. The abundance of AMPs can range from as low as 0.17 items/$m^3$ to as high as 5700 items/$m^3$ (Li et al., 2020c; Yuan et al., 2023; Zhu et al., 2021). MPs are more easily transported over long distances in the air compared to MPs in water or soil (Bullard et al., 2021; Zhang et al., 2019). The presence of AMPs in the pristine mountain (Allen et al., 2019), remote lake basin (Dong et al., 2021), and polar regions (Bergmann et al., 2019), indicates that the long-range atmospheric transport of MPs is substantial and should not be ignored. Anthropogenic activities in urban areas are the main source of AMPs (Evangeliou et al., 2022; Liu et al., 2019b). These pollutants can be transported over long distance, and their journey generally begins at the ground level. The transport of AMPs is a complex three-dimension process, involving both vertical and horizontal movement. Of the two, vertical transport plays a critical role in determining the distance of long-range transport (Kim et al., 2023; Zhen et al., 2021).

Evidence shows that AMPs can be transported vertically to higher levels (Allen et al., 2021; González-Pleiter et al., 2021). However, the vertical transport efficiency and mechanisms of AMPs are not fully understood. Generally, the vertical transport of pollutants from near-ground to higher altitudes is dynamically controlled by turbulence and convection, which are highly dependent on the thermal stratification within the atmospheric boundary layer (Miao et al., 2019; Petäjä et al., 2016). Temperature inversion can impede the upward diffusion of air pollutants from ground level, resulting in the accumulation of pollutants (Zhang et al., 2020a). The presence of an urban underlying surface can further complicate the diffusion of pollutants due to changes in atmospheric dynamics (Miao et al., 2019; Miao et al., 2015b). For instance, in densely populated and built-up urban areas, the atmospheric temperature at low altitudes may increase, which can change atmospheric stability and aggravate local air pollution (Miao et al., 2015a). Cities are often the source of MP pollution (Allen et al., 2019; Wright et al., 2020), so it is essential to understand the vertical distribution of AMPs on the urban underlying surface to better comprehend the long-range transport of AMPs.

Previous studies on air pollutants have utilized tethered balloons, aircraft, unmanned aerial vehicles, and meteorological towers to measure the vertical distribution of their concentrations (Liu et al., 2020; Manoj et al., 2020; Shi et al., 2022; Zhou et al., 2020). Although tethered balloons and unmanned aerial vehicles offer higher vertical resolution, their sample collection is limited by flight height and cannot be conducted for extended periods of time, such as 12 or 24 h. Furthermore, the sampler for active pumped sampling should remain energized during the sampling period (Liu et al., 2022; Shruti et al., 2022; Zhu et al., 2021), which leads to the fact that these methods are rarely considered in AMP studies. Aircraft sampling was applied in an AMP study in Spain, which revealed the presence of AMPs above the atmospheric boundary layer (González-Pleiter et al., 2021). However, the low altitude samples (<500 m) were not collected due to flight requirements, making it difficult to analyze the vertical distribution. To date, several studies have reported the occurrence of AMPs at different heights above the ground level, and the heights of these studies mostly depend on the terrain altitudes, such as mountains (Allen et al., 2019; González-Pleiter et al., 2021; Napper et al., 2020). However, the mountains are generally located far from urban areas, which cannot accurately reflect urban AMP pollution. Tower-based observation is a more effective approach to studying the vertical distribution of air pollutant concentrations in urban areas, which can provide the characteristics of pollutants at multiple heights. This method has been widely used in many studies over the last decade. For example, Lee et al. (2015) conducted a study on oxynitride ($NO_X$) concentration based on a 190 m tall BT tower located in central London. Sun et al. (2015) observed the interactions between the atmospheric boundary layer and aerosol chemistry on a 325 m meteorological tower situated in urban Beijing.

The Canton Tower, which is the tallest tower in China and is well-equipped with meteorological monitoring platforms and facilities, provides a unique platform to study the distribution and transport of AMPs in the atmospheric boundary layer. In this study, we measured the abundances and characteristics of AMPs at four different heights on the Canton Tower for the first time. Our aim was to describe the vertical profile of AMPs and investigate the effects of atmospheric layer structure and meteorological conditions on AMPs vertical transport within the atmospheric boundary layer.

## 2. Materials and methods

### 2.1. Study site and sampling method

The Canton Tower is located in urban Guangzhou, with a total height of 604 m (Fig. 1). Air quality monitoring stations of the Guangzhou Environmental Monitoring Center are established at the four heights of the Canton Tower (ground level, 118 m, 168 m and 488 m), which are also part of the

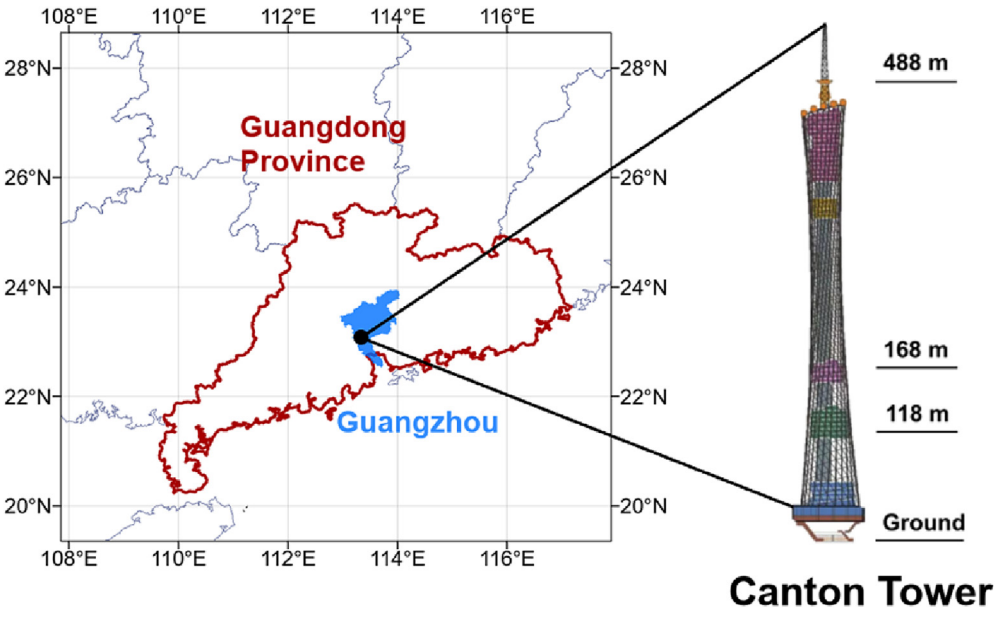


**Fig. 1.** Sampling sites at different heights of the Canton Tower in Guangzhou.

long-term urban air quality monitoring network in Guangzhou. The stations provide data regarding meteorological conditions and air quality at four heights. Meteorological parameters include temperature, wind direction, wind speed, rainfall, pressure, and relative humidity. Nitric oxide (NO), nitrogen dioxide ($NO_2$), $NO_X$, ozone ($O_3$), carbonic oxide (CO), sulfur dioxide ($SO_2$) and particulate matter ($PM_{2.5}$, $PM_1$) are among the eight typical air pollutants that are monitored every day. The study site is located in the urban center of Guangzhou; therefore, meteorological conditions and air quality at different heights can reflect the vertical atmospheric environment over the urban underlying surface.

This study is designed to analyze the vertical distribution and transport of AMPs in the atmosphere near the ground level by determining the AMP abundance at different altitudes. Air samples were collected at ground level, 118 m, 168 m and 488 m (above the ground level) of the tower, where the monitoring stations were situated, as shown in Fig. 1. The sampling was completed using a medium flow total suspended particle sampler (KB-6120, Jinshida, Qingdao) for two weeks (from Sep. 9th to Sep. 27th of 2021). Sampling was carried out every other day for 24 h, with an intake flow rate of 100 L/min. For sampling at 488 m, a small flow automatic film-changing particle sampler (PNS 16T-3.1, Comde-Derenda) was chosen specifically for the safety of working at altitudes. The three-week period of daily sampling (from Sep. 9th to Oct. 8th of 2021) was interrupted every day for five minutes to change the filters. All samples were collected on Whatman glass microfiber filters with a 1.6 μm pore size (47 mm and 90 mm in diameter for the middle and small flow samplers, respectively). After sampling, the folded filter was carefully wrapped by aluminum foils.

### 2.2. Quantification and verification of AMPs

Microplastics are generally uniform in color, light glossy and stretchy, with no cell or organic structures (Chen et al., 2020; Song et al., 2015). Based on these visual characteristics, the suspected MPs were selected under a microscope (Olympus SZX10, Japan). In the meantime, the characteristics of suspected MPs, including size, shape, and color, were photographed and recorded with an equipped digital camera (Olympus DP80, Japan) on the microscope.

Micro-Fourier Transform Infrared Spectroscopy (FTIR) analysis (Nicolet iN10, Thermo Fisher, U.S.A.) was used to verify the composition of MPs. The test condition is set to reflection mode, scanning 16 times per second with a resolution of 4 $cm^{-1}$. The composition of MPs could be identified by comparing the reflection spectra of each suspected MP with the built-in standard spectra library. According to previous studies, the component with a match >60 % could be regarded as the composition of the measured MP (Liu et al., 2019a; Yuan et al., 2023).

### 2.3. Quality assurance

To ensure impurity-free filters, all filters and laboratory supplies were baked for 4 h at 450 °C in a muffle furnace and covered in aluminum foil while not in use. During the procedure, the usage of plastic products was minimized. For example, the wire was used to fasten suspended particulate samplers instead of nylon rope. All metal or glass materials used were meticulously cleaned with Milli-Q water and covered in aluminum foil when not in use. An all-cotton lab coat, cotton mask, and nitrile gloves were always worn when working with samples in order to reduce contamination. Additionally, the lab doors and windows were kept closed. Three laboratory blanks were set in each of the steps for MP isolation and polymer identification in the laboratory. All six blank samples were free of MPs.

### 2.4. Data processing

Following previous studies (Allen et al., 2021; Wright et al., 2020), the aerodynamic diameter was adopted to describe the size of the AMPs, which was calculated using the following equation:

$$D \approx \left(d_p \ln 2\theta\right)^{1/2} D_P \quad (1)$$

In which $D$ is the aerodynamic diameter, $d_p$ is the density of the article, $\theta$ is the aspect ratio of particles and $D_P$ is the cylindrical diameter of particles.

The software packages Excel 2019 and SPSS 24.0 were used for all statistical analyses, and Origin 2020b was used to create the final graphs. In this study, the standard deviation (SD) was used to measure the fluctuation of the data and statistical significance was accepted at $p < 0.05$ in all statistical tests.

## 3. Results and discussion

### 3.1. Occurrence and characteristics of AMPs

Microplastics were detected in all samples (N = 52), and 198 of the 406 suspected AMPs were verified. Fig. 2a displays the time series of AMP abundances at various heights. Overall, the abundance of AMPs ranged from $4.20 \times 10^{-5}$ to 0.13 items/$m^3$, and slight fluctuations occurred in daily abundance at each height. The average abundances were 0.05 ± 0.03 items/$m^3$, 0.02 ± 0.01 items/$m^3$, 0.04 ± 0.02 items/$m^3$ and (1.12 ± 0.49) × $10^{-4}$ items/$m^3$ at ground level, 118 m, 168 m and 488 m, respectively. The sampling period included weekdays and weekends, with Sep. 11th, 12th, 18th, 19th, 25th, 26th and Oct. 2nd and 3rd being weekends. There were no significant differences in AMP abundance between weekdays and weekends in this study. However, these observations were far from the results obtained at 80 m (0.9 items/$m^3$) and 2500 m (13.9 items/$m^3$) above the city in previous studies (Liu et al., 2019a; González-Pleiter et al., 2021). The differences might be due to variances in study areas and sampling methods. The variety of different cities had a substantial impact on AMP abundances, which ranged from 1.42 items/$m^3$ to 5670 items/$m^3$ (Liu et al., 2019a; Li et al., 2020c). On the other hand, since there are currently no recognized uniform sampling and analytical protocols for AMPs, different methods may result in different results (Yuan et al., 2022). Even by a consistent sampling method, the AMP abundances in different cities could vary by up to six times (Zhu et al., 2021). Considering the city development level and weather change, the observations on AMPs may also fluctuate at different time. Therefore, it is not preferable to compare sampling results from different areas at different heights.

All AMPs observed in this study were in the shape of fibers, which is consistent with our findings of AMPs in Guangzhou throughout 2021 (Yuan et al., 2023). In previous studies, fiber is also considered the dominant shape of AMPs in urban areas, such as in urban Paris (fibers accounted for 90 %) (Dris et al., 2015), London (for 92 %) (Wright et al., 2020) and Dongguan (for 80 %) (Cai et al., 2017). A large aspect ratio of fibers could increase the air resistance in the opposite direction of gravity during descent, extending their atmospheric residence time (Bullard et al., 2021) and supporting the upward transport of AMPs. A study from London has also demonstrated that fibrous AMPs can travel further and have a larger potential influence area than non-fibrous AMPs, with a transport distance of 12 km for non-fibers and 60 km for fibers (Wright et al., 2020). Transparent and blue were the most popular colors in the measured AMPs, which were also the common colors found in previous studies (Liu et al., 2019a; Yuan et al., 2023). Black, red, green, and yellow were also observed (Fig. S1). The color can be the clue to trace the source. For example, the vivid colors such as blue and red are widely seen on textiles, while transparent are frequently utilized in packaged products (Zhang et al., 2019; Zhang et al., 2020b). However, the color of AMPs may fade or change during weathering or sample preparation, thus more features are required to pinpoint their source.

All of the AMPs that were found to have aerodynamic diameters <100 μm and 95 % of them to have diameters <60 μm, indicating that these AMPs could remain suspended in the environment. The predominant size range was 30– 50 μm, and AMPs with a smaller size (30– 40 μm) tended to be easier to raise higher, up to 488 m (Fig. 2c). The density of AMPs also influences their behavior in addition to size. The measured AMPs were comprised of rayon, cellophane, polymethyl methacrylate (PMMA), polyamide (PA), and polyethylene terephthalate (PET). Rayon and PET were

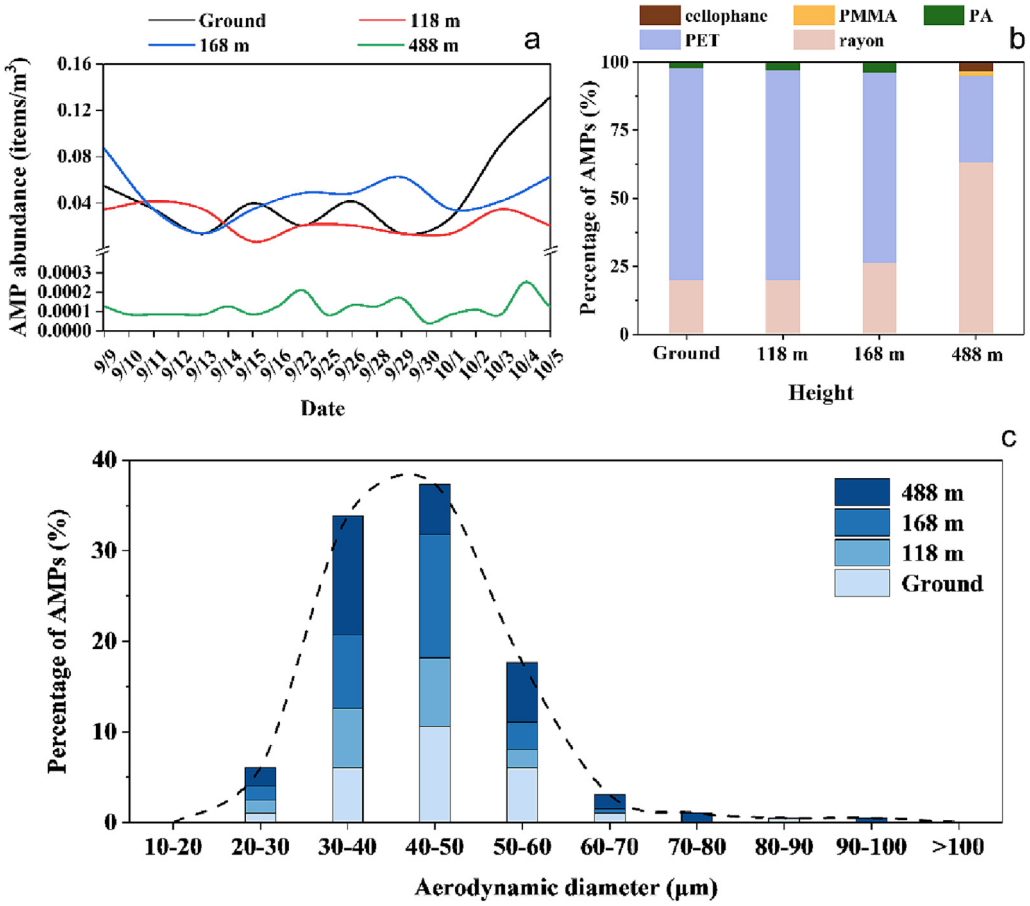


**Fig. 2.** Diurnal variations of AMP abundance at ground level, 118 m, 168 m, and 488 m (a), polymer type (b) and the composition of aerodynamic diameter (c). Polymer types are given by abbreviations. PMMA: polymethyl methacrylate; PA: polyamide; PET: polyethylene terephthalate.

the main polymer types, but the PET/rayon ratio decreased as the height increased (Fig. 2b). This may be related to the density of different materials. The major types of rayon fibers in this study were Kayocel and Natrosol 250, with densities of 0.75 g/cm$^3$ and 1.10 g/cm$^3$, respectively. With a density between 1.37 and 1.45 g/cm$^3$ (Hidalgo-Ruz et al., 2012), PET is heavier than rayon and therefore may restrict its upward movement.

### 3.2. Vertical profile of AMPs and relationships with other air pollutants

As shown in Fig. 2, AMPs were measured at each height and their abundance varied at different heights. There was little change in AMP abundance from ground level to 168 m. However, the abundance of AMPs at 488 m dramatically dropped by two orders of magnitude in comparison to the abundance at ground level (Kruskal-Wallis test, $p < 0.05$). The abundance of AMP did not simply decrease linearly with height, but has different change rates at different altitude layers. Fig. 3 depicts the vertical profiles of AMP abundance and common air pollutant concentrations based on tower observations. As the height to the ground level increased, AMP abundance fell from 0.05 ± 0.03 items/m$^3$ at ground level to 0.02 ± 0.01 items/m$^3$ at 118 m. At 168 m, there was a rise in AMP abundance. Despite the elevated trend, the abundance at 168 m was still lower than the ground-level abundance. As the height continued to increase, there was another obvious downward trend in the abundance of AMPs.

In general, meteorological factors, source emissions and atmospheric dispersion are the main factors that affect the vertical distribution of air pollutants, among which AMPs are included. Because there was no rainfall

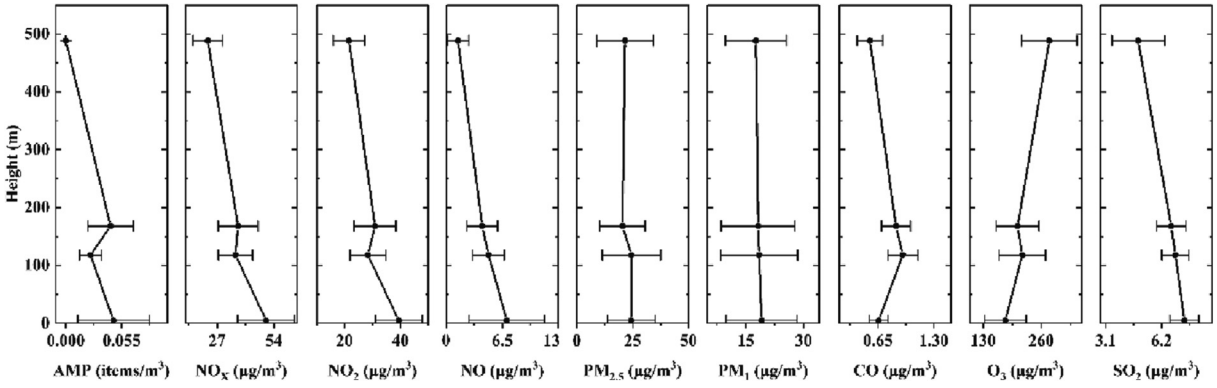


**Fig. 3.** Vertical profiles of AMPs and common air pollutants, including $NO_X$, $NO_2$, NO, $PM_{2.5}$, $PM_1$, CO, $O_3$ and $SO_2$.

during the monitoring periods, the resulting vertical abundance represented a typical vertical profile of AMPs in the urban area. The average height of buildings in Guangzhou is 43.3 m (Chen et al., 2021), indicating that human activities occur within this height. And industrial production and living activities are the main sources of AMPs, such as tire wear and tear, textile shedding, and the usage of cosmetics and plastic containers (Cai et al., 2021; Du et al., 2020; Evangeliou et al., 2020; Napper et al., 2015). This might account for the high abundance of AMPs measured at ground level. The source of AMPs generally declines as altitude increases, resulting in a declining trend in AMP abundance. Specifically, the Canton Tower, a popular tourist attraction, has an aerial climbing project for recreation at 168 m, and friction between visitors' clothing and the safety rope when climbing activities can release fibers (Napper et al., 2020). Near the 168 m climbing platform, samples of 10 different ropes were collected and examined their polymer compositions (Table S1). The main polymer types were rayon and PET, which was in line with AMP polymer types at 168 m. Therefore, the climbing activities may be one of the reasons for the elevated abundance of AMP abundance at 168 m. In addition to pollution sources, atmospheric dispersion comprises vertical convection and advection, which greatly govern the long-range transport of air pollutants (Kim et al., 2023). Vertical convection and advection are affected by the thermodynamic structure of the atmosphere and wind, which is discussed in detail in Section 3.3.

Previous studies have revealed that there is no correlation between the temporal distribution of AMP abundance and the concentrations of common air pollutants (Yuan et al., 2023; Zhu et al., 2021). However, we found some similarities in their vertical distribution. With the exception of $O_3$, the concentrations of $NO_X$, $NO_2$, NO, $PM_{2.5}$, $PM_1$, CO and $SO_2$ exhibited a general decreasing trend from ground to 488 m height, but the decreasing rate varied (Fig. 3). This may be related to the characteristics of different pollutants. Since the ultraviolet radiation at 300– 500 m is generally stronger than that at ground level, photochemical reactions will result in a rise in the concentration of $O_3$ (He et al., 2021). Li et al. (2020a) also demonstrated that photochemical processes were the primary cause of the Pearl River Delta's elevated $O_3$ content at higher altitudes. For atmospheric particles, both AMP and particulate matter ($PM_{2.5}$ and $PM_1$) decreased in abundance with height, although the rate of decrease was faster for AMPs. This may be related to their particle size. Deng et al. (2015) measured the particulate matter ($PM_{10}$, $PM_{2.5}$ and $PM_1$) at different heights on the Canton Tower and found that finer particles had a more uniform vertical distribution than coarse particles. Our field observations are consistent with this rule. The vertical reduction in AMP abundance was more noticeable than that of $PM_{2.5}$ and $PM_1$ because AMPs were primarily in size range of 30– 50 μm. It is interesting to note that the vertical profiles of AMPs and $NO_X$ showed the similar pattern. The elevated $NO_X$ concentration at high altitudes was commonly caused by atmospheric input from

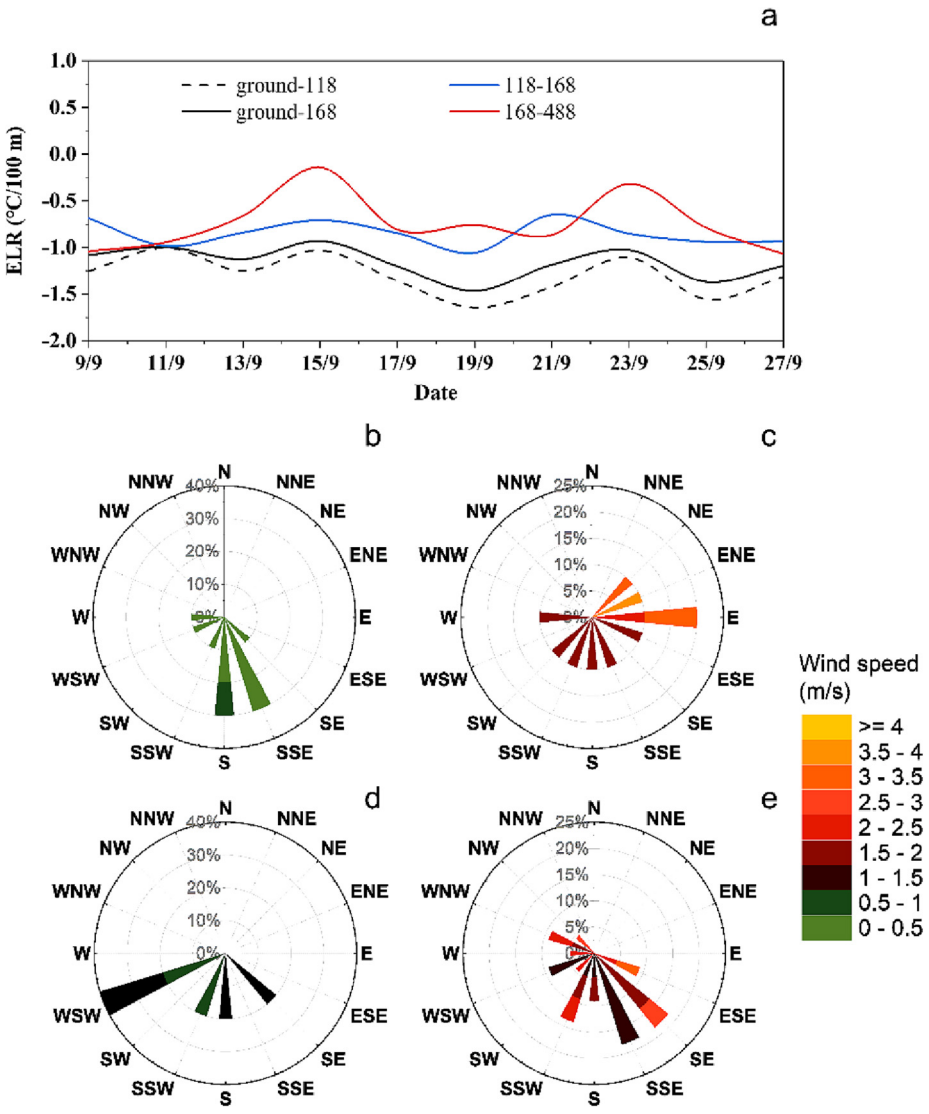


**Fig. 4.** Variations in environmental lapse rates (ELR) (a) and wind rose plots at ground level (b), 118 m (c), 168 m (d), and 488 m (e) in September 2021.

surrounding areas (Wang et al., 2023). Similarly, the elevation of AMP abundance at 168 m may also be related to peripheral inputs, which needs to be proven by more evidence.

### 3.3. Effects of atmospheric stability and wind on the vertical distribution of AMPs

#### 3.3.1. Atmospheric stability

Atmospheric stability is commonly used to describe the ability of air masses to move vertically, which strongly affects the dispersion and accumulation of air pollutants (Liu et al., 2020; Sun et al., 2023). The atmospheric stability can be described by the environmental lapse rate (ELR), which is defined as the decreasing rate of temperature with rising altitude. An ELR below the dry adiabatic lapse rate (DALR) of 9.8 °C/km indicates a stable atmosphere, which limits atmospheric convective motion (Chan et al., 2005). Fig. 4a displays the atmospheric stability conditions at different altitude layers during the monitoring period. There was no strong temperature inversion, implying that AMPs could be carried vertically to higher levels as the air mass rose under the effect of thermodynamics. Strong convective activity was typically present along with the unstable atmospheric stability from the ground level to 118 m (Chen et al., 2022), and this helped to facilitate the vertical diffusion of AMPs. However, the ELRs from 118 m to 168 m and 168 m to 488 m frequently fell below the DALR of 9.8 °C/km as the height increased. As a result, the vertical diffusion of AMPs was prevented at higher atmospheres (>118 m) where the convection intensity was weaker. Critically, a relatively stable fine layer that inhibited the upward movement of AMPs between 118 m and 168 m was evident from the fact that almost all ELRs between 118 m and 168 m were lower than the DALR.

The height of the atmospheric boundary layer may also influence the vertical distribution of air pollutants (Li et al., 2020b). The formation of atmospheric boundary layer was not favored by a smaller temperature gradient or thermal inversion, and a lower atmospheric boundary layer would prevent the transfer of more air pollutants from low levels to high levels (Miao et al., 2021). For instance, the ELR between 168 m and 488 m on September 15 was close to zero (Fig. 4a), suggesting that AMPs might be trapped below in the lower troposphere (<488 m) and could not be transported to higher levels. The lower AMP abundance values observed on September 15 at 488 m also support this assumption (Fig. 2a).

#### 3.3.2. Wind

In addition to the thermal impacts, mechanical impacts from wind conditions can also alter the vertical distribution of AMPs (Liang et al., 2022; Sun et al., 2015). In September, Guangzhou experiences a predominantly southerly wind. There were no highly unusual wind directions at any heights (Fig. 4b–e), and the wind direction was primarily southerly. At 168 m, west-southwest (WSW) winds were most prevalent, but this predominant wind direction did not coincide with the high AMP abundance, suggesting that the WSW wind was not the primary factor in the high AMP abundance. Even at 118 m, which was close to 168 m, the AMP pollution was found to be abated in the prevailing western or WSW winds (Fig. 4c) (Spearman's correlation, $r = -0.73$, $p < 0.05$). However, it was clear that the wind speed at 168 m was lower than that at 118 m, revealing that the impact of wind on the AMP vertical distribution is mainly caused by wind speed. Low wind speeds at ground level (Fig. 4b) caused AMPs at that altitude to largely move vertically with increasing air masses as a result of the thermodynamic effect, with limited horizontal diffusion. The reduced AMP abundance at 488 m (Fig. 4e) could also potentially be due to the comparatively high wind speed. Our findings are similar with other research that found a negative association between AMP abundance and wind speed (Ding et al., 2022; Liu et al., 2019a).

In conclusion, the vertical distribution of AMPs is largely determined by the combined impacts of atmospheric stability and wind speed. Intensity of vertical transport from the ground to higher altitudes is influenced by atmospheric stability, whereas horizontal diffusion is mostly affected by wind speed. As shown in Fig. 5, AMPs can be transported from ground level to approximately 100 m due to the effect of atmospheric thermodynamics. However, a fine layer is observed between 118 m and 168 m, in which the ELRs are small, indicating that the vertical transport of AMPs is restricted. The stability of the layer between 100 and 200 m, which creates a local concentration peak and distorts the trend of pollutants decreasing with height, has also been seen in previous measurements of urban vertical air conditions (Sun et al., 2015; Zhou et al., 2020). Furthermore, the calm wind may also contribute to AMP accumulation at 168 m. However, since the temperature within the atmospheric boundary layer decreases with height (Zhou et al., 2020), some of the AMPs may still be transported to higher altitudes. The transport of AMPs can be roughly divided into two stages: the atmospheric boundary layer stage and the free tropospheric layer stage. AMPs may primarily move in a turbulent manner within the atmospheric boundary layer, while long-range transport is feasible when they are delivered into the free troposphere layer (Lee et al., 2019). And it has been proven that AMPs can travel over 1000 km in the free troposphere layer (Allen et al., 2021; González-Pleiter et al., 2021).

Our results initially reveal the vertical transport of AMPs within the atmospheric boundary layer, although we are unable to dynamically monitor

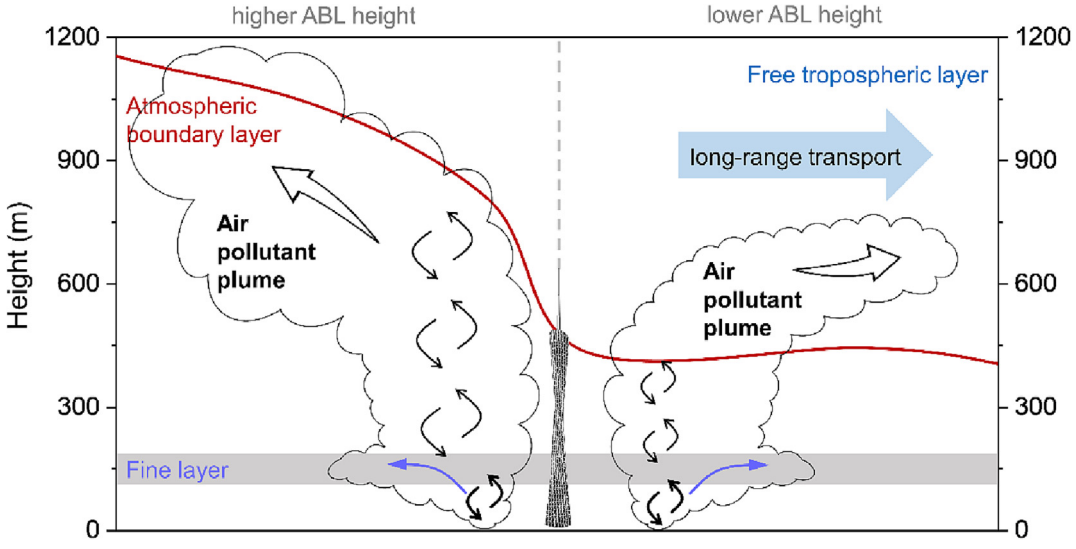


**Fig. 5.** Illustration of AMP vertical transport above the urban underlying surface. The fine layer occurs between 100 m and 200 m, where the vertical dispersion of AMPs is suppressed.

the vertical distribution of AMPs in the whole atmospheric boundary layer due to field limitations. Furthermore, the vertical transport processes of air pollutants above the urban underlying surface are of great complexity and may also be influenced by other factors. In central city areas, high-rise and dense buildings form deep street canyons that affect the vertical dispersion of air pollutants (Huang et al., 2021). For instance, the vortex induced by buildings confines air pollutants in street canyons (Chan and Kwok, 2000). Different roof shapes may also alter the flow field of the atmosphere, thus affecting the dispersion of pollutants (Ding et al., 2019). Therefore, more field vertical monitoring with high precision is needed to parameterize the vertical transport process of AMPs.

## 4. Conclusion

In this study, the abundances and characteristics of AMPs were measured at four heights (ground level, 118 m, 168 m and 488 m) of the Canton Tower in Guangzhou. Fibers were the main shapes of AMPs in urban Guangzhou, with a predominant size range of 30– 50 μm. Rayon and PET accounted for 95 % of polymer types, and the share of rayon at the higher altitude (488 m) increased obviously. Overall, AMP abundance showed a decreasing trend with height, but there was a local peak in AMP abundance at 168 m. The vertical profiles of AMPs and common air pollutants (including $NO_X$, $NO_2$, NO, $PM_{2.5}$, $PM_1$, CO, $O_3$, and $SO_2$) are similar in that they both contain a complicated fine layer between 118 m and 168 m. Atmospheric stability and wind are suggested to be the main causes of the vertical layered structures of AMPs in urban Guangzhou. Unstable atmospheric conditions were considered to be the driving force for the vertical dispersion of AMPs, while stable atmospheric stability between 118 m and 168 m could impede the vertical dispersion of air pollutants, including AMPs. On the other hand, the fine layer between 118 m and 168 m might also be associated with lower wind speeds (1 m/s at 168 m), which might promote the local accumulation of AMPs. The differences in the vertical distribution of different air pollutants may be due to their characteristics.

Our observations reported the characteristics and vertical profile of AMPs below 500 m and the factors affecting the AMP vertical profile. However, more field observations with a finer vertical resolution are still needed in the future to accurately model the vertical transport process of AMPs.

## CRediT authorship contribution statement

**Zhen Yuan:** Investigation, Formal analysis, Visualization, Writing – original draft, Writing – review & editing. **Cheng-Lei Pei:** Investigation, Resources. **Heng-Xiang Li:** Methodology. **Lang Lin:** Investigation. **Rui Hou:** Writing – review & editing. **Shan Liu:** Visualization. **Kai Zhang:** Writing – review & editing. **Ming-Gang Cai:** Funding acquisition, Supervision. **Xiang-Rong Xu:** Funding acquisition, Conceptualization, Supervision.

## Data availability

Data will be made available on request.

## Declaration of competing interest

The authors declare that they have no known competing financial interests or personal relationships that could have appeared to influence the work reported in this paper.

## Acknowledgment

This work was supported jointly by Hainan Province Science and Technology Special Fund (No. ZDYF2022SHFZ317), the National Natural Science Foundation of China (Nos. U2005207, 42206149, U21A2036), Natural Science Foundation of Hainan Province (No. 422QN443), The Science and Technology Planning Project of Guangdong Province, China (No. 2020B1212060058).

## Appendix A. Supplementary data

Supplementary data to this article can be found online at https://doi.org/10.1016/j.scitotenv.2023.165190.

## References

Allen, S., Allen, D., Phoenix, V.R., Le Roux, G., Durántez, Jiménez P., Simonneau, A., Binet, S., Galop, D., 2019. Atmospheric transport and deposition of microplastics in a remote mountain catchment. Nat. Geosci. 12, 339–344. https://doi.org/10.1038/s41561-019-0335-5.

Allen, S., Allen, D., Baladima, F., Phoenix, V.R., Thomas, J.L., Le Roux, G., Sonke, J.E., 2021. Evidence of free tropospheric and long-range transport of microplastic at Pic du Midi Observatory. Nat. Commun. 12, 7242. https://doi.org/10.1038/s41467-021-27454-7.

Bergmann, M., Mützel, S., Primpke, S., Tekman, M.B., Trachsel, J., Gerdts, G., 2019. White and wonderful? Microplastics prevail in snow from the Alps to the Arctic. Sci. Adv. 5, eaax1157. https://doi.org/10.1126/sciadv.aax1157.

Bullard, J.E., Ockelford, A., O'Brien, P., McKenna, Neuman C., 2021. Preferential transport of microplastics by wind. Atmos. Environ. 245, 118038. https://doi.org/10.1016/j.atmosenv.2020.118038.

Cai, L.Q., Wang, J.D., Peng, J.P., Tan, Z., Zhan, Z.W., Tan, X.L., Chen, Q.Q., 2017. Characteristic of microplastics in the atmospheric fallout from Dongguan city, China: preliminary research and first evidence. Environ. Sci. Pollut. R. 24, 24928–24935. https://doi.org/10.1007/s11356-017-0116-x.

Cai, Y.P., Mitrano, D.M., Hufenus, R., Nowack, B., 2021. Formation of fiber fragments during abrasion of polyester textiles. Environ. Sci. Technol. 55, 8001–8009. https://doi.org/10.1021/acs.est.1c00650.

Chan, L.Y., Kwok, W.S., 2000. Vertical dispersion of suspended particulates in urban area of Hong Kong. Atmos. Environ. 34, 4403–4412. https://doi.org/10.1016/S1352-2310(00)00181-3.

Chan, C.Y., Xu, X.D., Li, Y.S., Wong, K.H., Ding, G.A., Chan, L.Y., Cheng, X.H., 2005. Characteristics of vertical profiles and sources of PM2.5, PM10 and carbonaceous species in Beijing. Atmos. Environ. 39, 5113–5124. https://doi.org/10.1016/j.atmosenv.2005.05.009.

Chen, G.L., Fu, Z.L., Yang, H.R., Wang, J., 2020. An overview of analytical methods for detecting microplastics in the atmosphere. TrAC Trends Anal. Chem. 130, 115981. https://doi.org/10.1016/j.trac.2020.115981.

Chen, B.Y., Wang, W.W., Dai, W., Chang, M., Wang, X.M., You, Y.C., Zhu, W.X., Liao, C.G., 2021. Refined urban canopy parameters and their impacts on simulation of urbanization-induced climate change. Urban Clim. 37, 100847. https://doi.org/10.1016/j.uclim.2021.100847.

Chen, L., Pang, X.B., Li, J.J., Xing, B., An, T.C., Yuan, K.B., Dai, S., Wu, Z.T., Wang, S.Q., Wang, Q., Mao, Y.P., Chen, J.M., 2022. Vertical profiles of O3, NO2 and PM in a major fine chemical industry park in the Yangtze River Delta of China detected by a sensor package on an unmanned aerial vehicle. Sci. Total Environ. 845, 157113. https://doi.org/10.1016/j.scitotenv.2022.157113.

Deng, X.J., Li, F., Li, Y.H., Li, J.Y., Huang, H.Z., Liu, X.T., 2015. Vertical distribution characteristics of PM in the surface layer of Guangzhou. Particuology 20, 3–9. https://doi.org/10.1016/j.partic.2014.02.009.

Ding, S., Huang, Y.D., Cui, P.Y., Wu, J., Li, M.Z., Liu, D.T., 2019. Impact of viaduct on flow reversion and pollutant dispersion in 2d urban street canyon with different roof shapes - numerical simulation and wind tunnel experiment. Sci. Total Environ. 671, 976–991. https://doi.org/10.1016/j.scitotenv.2019.03.391.

Ding, J.F., Sun, C.J., He, C.F., Zheng, L., Dai, D.J., Li, F.M., 2022. Atmospheric microplastics in the Northwestern Pacific Ocean: distribution, source, and deposition. Sci. Total Environ. 829, 154337. https://doi.org/10.1016/j.scitotenv.2022.154337.

Dong, H.K., Wang, L.X., Wang, X.P., Xu, L., Chen, M.K., Gong, P., Wang, C.F., 2021. Microplastics in a remote lake basin of the Tibetan Plateau: Impacts of atmospheric transport and glacial melting. Environ. Sci. Technol. 55, 12951–12960. https://doi.org/10.1021/acs.est.1c03227.

Dris, R., Gasperi, J., Rocher, V., Saad, M., Renault, N., Tassin, B., 2015. Microplastic contamination in an urban area: a case study in greater Paris. Environ. Chem. 12, 592–599. https://doi.org/10.1071/EN14167.

Du, F.N., Cai, H.W., Zhang, Q., Chen, Q.Q., Shi, H.H., 2020. Microplastics in take-out food containers. J. Hazard. Mater. 399, 122969. https://doi.org/10.1016/j.jhazmat.2020.122969.

Evangeliou, N., Grythe, H., Klimont, Z., Heyes, C., Eckhardt, S., Lopez-Aparicio, S., Stohl, A., 2020. Atmospheric transport is a major pathway of microplastics to remote regions. Nat. Commun. 11, 3381. https://doi.org/10.1038/s41467-020-17201-9.

Evangeliou, N., Tichý, O., Eckhardt, S., Zwaaftink, C.G., Brahney, J., 2022. Sources and fate of atmospheric microplastics revealed from inverse and dispersion modelling: from global emissions to deposition. J. Hazard. Mater. 432, 128585. https://doi.org/10.1016/j.jhazmat.2022.128585.

González-Pleiter, M., Edo, C., Aguilera, Á., Viúdez-Moreiras, D., Pulido-Reyes, G., González-Toril, E., Osuna, S., de Diego-Castilla, G., Leganés, F., Fernández-Piñas, F., Rosal, R., 2021. Occurrence and transport of microplastics sampled within and above the planetary boundary layer. Sci. Total Environ. 761, 143213. https://doi.org/10.1016/j.scitotenv.2020.143213.

He, G.W., Deng, T., Wu, D., Wu, C., Huang, X.F., Li, Z.N., Yin, C.Q., Zou, Y., Song, L., Ouyang, S.S., Tao, L.P., Zhang, X., 2021. Characteristics of boundary layer ozone and its effect on surface ozone concentration in Shenzhen, China: a case study. Sci. Total Environ. 791, 148044. https://doi.org/10.1016/j.scitotenv.2021.148044.

Hidalgo-Ruz, V., Gutow, L., Thompson, R.C., Thiel, M., 2012. Microplastics in the marine environment: a review of the methods used for identification and quantification. Environ. Sci. Technol. 46, 3060–3075. https://doi.org/10.1021/es2031505.

Huang, Y.H., Lei, C.W., Liu, C.H., Perez, P., Forehead, H., Kong, S., Zhou, J.L., 2021. A review of strategies for mitigating roadside air pollution in urban street canyons. Environ. Pollut. 280, 116971. https://doi.org/10.1016/j.envpol.2021.116971.

Kim, E., Kim, B.U., Kang, Y.H., Kim, H.C., Kim, S., 2023. Role of vertical advection and diffusion in long-range PM2.5 transport in Northeast Asia. Environ. Pollut. 320, 120997. https://doi.org/10.1016/j.envpol.2022.120997.

Lee, J.D., Helfter, C., Purvis, R.M., Beevers, S.D., Carslaw, D.C., Lewis, A.C., Møller, S.J., Tremper, A., Vaughan, A., Nemitz, E.G., 2015. Measurement of nox fluxes from a tall tower in central London, UK and comparison with emissions inventories. Environ. Sci. Technol. 49, 1025–1034. https://doi.org/10.1021/es5049072.

Lee, H.J., Jo, H.Y., Kim, S.W., Park, M.S., Kim, C.H., 2019. Impacts of atmospheric vertical structures on transboundary aerosol transport from China to South Korea. Sci. Rep. 9, 13040. https://doi.org/10.1038/s41598-019-49691-z.

Li, L., Lu, C., Chan, P.W., Zhang, X., Yang, H.L., Lan, Z.J., Zhang, W.H., Liu, Y.W., Pan, L., Zhang, L., 2020a. Tower observed vertical distribution of PM2.5, O3 and NOx in the Pearl River Delta. Atmos. Environ. 220, 117083. https://doi.org/10.1016/j.atmosenv.2019.117083.

Li, Q.H., Wu, B.H., Liu, J.L., Zhang, H.S., Cai, X.H., Song, Y., 2020b. Characteristics of the atmospheric boundary layer and its relation with pm2.5 during haze episodes in winter in the North China plain. Atmos. Environ. 223, 117265. https://doi.org/10.1016/j.atmosenv.2020.117265.

Li, Y.W., Shao, L.Y., Wang, W.H., Zhang, M.Y., Feng, X.L., Li, W.J., Zhang, D.Z., 2020c. Airborne fiber particles: types, size and concentration observed in Beijing. Sci. Total Environ. 705, 135967. https://doi.org/10.1016/j.scitotenv.2019.135967.

Liang, Y., Wu, C., Wu, D., Liu, B., Li, Y.J., Sun, J., Yang, H., Mao, X., Tan, J., Xia, R., Deng, T., Li, M., Zhou, Z., 2022. Vertical distributions of atmospheric black carbon in dry and wet seasons observed at a 356-m meteorological tower in Shenzhen, South China. Sci. Total Environ. 853, 158657. https://doi.org/10.1016/j.scitotenv.2022.158657.

Liu, K., Wang, X.H., Fang, T., Xu, P., Zhu, L.X., Li, D.J., 2019a. Source and potential risk assessment of suspended atmospheric microplastics in Shanghai. Sci. Total Environ. 675, 462–471. https://doi.org/10.1016/j.scitotenv.2019.04.110.

Liu, K., Wu, T.N., Wang, X.H., Song, Z.Y., Zong, C.X., Wei, N., Li, D.J., 2019b. Consistent transport of terrestrial microplastics to the ocean through atmosphere. Environ. Sci. Technol. 53, 10612–10619. https://doi.org/10.1021/acs.est.9b03427.

Liu, B., Wu, C., Ma, N., Chen, Q., Li, Y.W., Ye, J.H., Martin, S.T., Li, Y.J., 2020. Vertical profiling of fine particulate matter and black carbon by using unmanned aerial vehicle in Macau, China. Sci. Total Environ. 709, 136109. https://doi.org/10.1016/j.scitotenv.2019.136109.

Liu, Z., Huang, Q.E., Chen, L., Li, J.H., Jia, H.Z., 2022. Is the impact of atmospheric microplastics on human health underestimated? Uncertainty in risk assessment: a case study of urban atmosphere in Xi'an, Northwest China. Sci. Total Environ. 158167. https://doi.org/10.1016/j.scitotenv.2022.158167.

Manoj, M.R., Satheesh, S.K., Moorthy, K.K., Coe, H., 2020. Vertical profiles of submicron aerosol single scattering albedo over the indian region immediately before monsoon onset and during its development: research from the swaami field campaign. Atmos. Chem. Phys. 20, 4031–4046. https://doi.org/10.5194/acp-20-4031-2020.

Miao, Y.C., Liu, S.H., Zheng, Y.J., Wang, S., Chen, B.C., Zheng, H., Zhao, J.C., 2015a. Numerical study of the effects of local atmospheric circulations on a pollution event over Beijing–Tianjin–Hebei, China. J. Environ. Sci. 30, 9–20. https://doi.org/10.1016/j.jes.2014.08.025.

Miao, Y.C., Liu, S.H., Zheng, Y.J., Wang, S., Liu, Z.X., Zhang, B.H., 2015b. Numerical study of the effects of planetary boundary layer structure on the pollutant dispersion within built-up areas. J. Environ. Sci. 32, 168–179. https://doi.org/10.1016/j.jes.2014.10.025.

Miao, Y.C., Li, J., Miao, S.G., Che, H.Z., Wang, Y.Q., Zhang, X.Y., Zhu, R., Liu, S.H., 2019. Interaction between planetary boundary layer and PM2.5 pollution in megacities in China: a review. Curr. Pollut. Rep. 5, 261–271. https://doi.org/10.1007/s40726-019-00124-5.

Miao, Y.C., Che, H.Z., Zhang, X.Y., Liu, S.H., 2021. Relationship between summertime concurring PM2.5 and O3 pollution and boundary layer height differs between Beijing and Shanghai, China. Environ. Pollut. 268, 115775. https://doi.org/10.1016/j.envpol.2020.115775.

Napper, I.E., Bakir, A., Rowland, S.J., Thompson, R.C., 2015. Characterisation, quantity and sorptive properties of microplastics extracted from cosmetics. Mar. Pollut. Bull. 99, 178–185. https://doi.org/10.1016/j.marpolbul.2015.07.029.

Napper, I.E., Davies, B.F.R., Clifford, H., Elvin, S., Koldewey, H.J., Mayewski, P.A., Miner, K.R., Potocki, M., Elmore, A.C., Gajurel, A.P., Thompson, R.C., 2020. Reaching new heights in plastic pollution—preliminary findings of microplastics on Mount Everest. One Earth. 3, 621–630. https://doi.org/10.1016/j.oneear.2020.10.020.

Petäjä, T., Järvi, L., Kerminen, V.M., Ding, A.J., Sun, J.N., Nie, W., Kujansuu, J., Virkkula, A., Yang, X., Fu, C.B., Zilitinkevich, S., Kulmala, M., 2016. Enhanced air pollution via aerosol-boundary layer feedback in China. Sci. Rep. 6, 18998. https://doi.org/10.1038/srep18998.

Shi, Y.J., Wang, D.F., Huo, J.T., Duan, Y.S., Lin, Y.F., Huang, K., Fu, Q.Y., Xiu, G.L., 2022. Vertically-resolved sources and secondary formation of fine particles: a high resolution tethered mega-balloon study over Shanghai. Sci. Total Environ. 802, 149681. https://doi.org/10.1016/j.scitotenv.2021.149681.

Shruti, V.C., Kutralam-Muniasamy, G., Pérez-Guevara, F., Roy, P.D., Martínez, I.E., 2022. Occurrence and characteristics of atmospheric microplastics in Mexico city. Sci. Total Environ. 847, 157601. https://doi.org/10.1016/j.scitotenv.2022.157601.

Song, Y.K., Hong, S.H., Jang, M., Han, G.M., Rani, M., Lee, J., Shim, W.J., 2015. A comparison of microscopic and spectroscopic identification methods for analysis of microplastics in environmental samples. Mar. Pollut. Bull. 93, 202–209. https://doi.org/10.1016/j.marpolbul.2015.01.015.

Sun, Y.L., Du, W., Wang, Q.Q., Zhang, Q., Chen, C., Chen, Y., Chen, Z.Y., Fu, P.Q., Wang, Z.F., Gao, Z.Q., Worsnop, D.R., 2015. Real-time characterization of aerosol particle composition above the urban canopy in Beijing: insights into the interactions between the atmospheric boundary layer and aerosol chemistry. Environ. Sci. Technol. 49, 11340–11347. https://doi.org/10.1021/acs.est.5b02373.

Sun, X.Y., Zhao, T.L., Tang, G.Q., Bai, Y.Q., Kong, S.F., Zhou, Y., Hu, J., Tan, C.H., Shu, Z.Z., Xu, J.P., Ma, X.D., 2023. Vertical changes of pm2.5 driven by meteorology in the atmospheric boundary layer during a heavy air pollution event in Central China. Sci. Total Environ. 858, 159830. https://doi.org/10.1016/j.scitotenv.2022.159830.

Wang, Y.J., Liu, J.W., Jiang, F., Chen, Z.X., Wu, L.L., Zhou, S.Z., Pei, C.L., Kuang, Y., Cao, F., Zhang, Y.L., Fan, M.Y., Zheng, J.Y., Li, J., Zhang, G., 2023. Vertical measurements of stable nitrogen and oxygen isotope composition of fine particulate nitrate aerosol in Guangzhou city: source apportionment and oxidation pathway. Sci. Total Environ. 865, 161239. https://doi.org/10.1016/j.scitotenv.2022.161239.

Wright, S.L., Ulke, J., Font, A., Chan, K.L.A., Kelly, F.J., 2020. Atmospheric microplastic deposition in an urban environment and an evaluation of transport. Environ. Int. 136, 105411. https://doi.org/10.1016/j.envint.2019.105411.

Yuan, Z., Li, H.X., Lin, L., Pan, Y.F., Liu, S., Hou, R., Xu, X.R., 2022. Occurrence and human exposure risks of atmospheric microplastics: a review. Gondwana Res. 108, 200–212. https://doi.org/10.1016/j.gr.2022.02.001.

Yuan, Z., Pei, C.L., Li, H.X., Lin, L., Liu, S., Hou, R., Liao, R., Xu, X.R., 2023. Atmospheric microplastics at a Southern China metropolis: occurrence, deposition flux, exposure risk and washout effect of rainfall. Sci. Total Environ. 869, 161839. https://doi.org/10.1016/j.scitotenv.2023.161839.

Zhang, Y.L., Gao, T.G., Kang, S.C., Sillanpää, M., 2019. Importance of atmospheric transport for microplastics deposited in remote areas. Environ. Pollut. 254, 112953. https://doi.org/10.1016/j.envpol.2019.07.121.

Zhang, K., Zhou, L., Fu, Q.Y., Yan, L., Morawska, L., Jayaratne, R., Xiu, G.L., 2020a. Sources and vertical distribution of PM2.5 over Shanghai during the winter of 2017. Sci. Total Environ. 706, 135683. https://doi.org/10.1016/j.scitotenv.2019.135683.

Zhang, Q., Zhao, Y.P., Du, F.N., Cai, H.W., Wang, G.H., Shi, H.H., 2020b. Microplastic fallout in different indoor environments. Environ. Sci. Technol. 54, 6530–6539. https://doi.org/10.1021/acs.est.0c00087.

Zhen, Z.X., Yin, Y., Chen, K., Zhen, X.L., Zhang, X., Jiang, H., Wang, H.L., Kuang, X., Cui, Y., Dai, M.M., He, C., Liu, A.K., Zhou, F.H., 2021. Concentration and atmospheric transport of pm2.5-bound polycyclic aromatic hydrocarbons at Mount Tai, China. Sci. Total Environ. 786, 147513. https://doi.org/10.1016/j.scitotenv.2021.147513.

Zhou, S.Z., Wu, L.L., Guo, J.C., Chen, W.H., Wang, X.M., Zhao, J., Cheng, Y.F., Huang, Z.Z., Zhang, J.P., Sun, Y.L., Fu, P.Q., Jia, S.G., Tao, J., Chen, Y.N., Kuang, J.X., 2020. Measurement report: vertical distribution of atmospheric particulate matter within the urban boundary layer in Southern China – size-segregated chemical composition and secondary formation through cloud processing and heterogeneous reactions. Atmos. Chem. Phys. 20, 6435–6453. https://doi.org/10.5194/acp-20-6435-2020.

Zhu, X., Huang, W., Fang, M.Z., Liao, Z.L., Wang, Y.Q., Xu, L.S., Mu, Q.Q., Shi, C.W., Lu, C.J., Deng, H.H., Dahlgren, R., Shang, X., 2021. Airborne microplastic concentrations in five megacities of Northern and Southeast China. Environ. Sci. Technol. https://doi.org/10.1021/acs.est.1c03618.